We are IntechOpen,
the world's leading publisher of
Open Access books
Built by scientists, for scientists

6,900
Open access books available

185,000
International authors and editors

200M
Downloads

154
Countries delivered to

Our authors are among the

TOP 1%
most cited scientists

12.2%
Contributors from top 500 universities

BOOK CITATION INDEX
CLARIVATE ANALYTICS
INDEXED

WEB OF SCIENCE™

Selection of our books indexed in the Book Citation Index
in Web of Science™ Core Collection (BKCI)

Interested in publishing with us?
Contact book.department@intechopen.com

Numbers displayed above are based on latest data collected.
For more information visit www.intechopen.com

Chapter

Influence of Al$_2$O$_3$ Processing on the Microtexture and Morphology of Mold Steel: Hydrophilic-to-Hydrophobic Transition

Kelvii Wei Guo

Abstract

The surface of mold steel was processed by the simple Al$_2$O$_3$ surface processing, and the influence of processing time on the surface morphology was studied by 3D profilometer and scanning electron microscopy (SEM). Moreover, the wettability of the Al$_2$O$_3$ microtextured surfaces of mold steel was also investigated. The results show that the surface morphology of mold steel varies with Al$_2$O$_3$ processing time. It reveals that the initial surface without any Al$_2$O$_3$ processing treatment behaves as a hydrophilic surface. With the increment of Al$_2$O$_3$ processing time, the surface roughness of the processed surface with the microtextures increases correspondingly. At the same time, the wettability of the microtextured surfaces changes from the hydrophilic to the hydrophobic. When Al$_2$O$_3$ processing time reaches 60 min, the contact angle reaches its maximum at which the relevant surface roughness is the minimum. It indicates that mold steel with an Al$_2$O$_3$ microtextured surface can be a potential application in the mold releasement.

Keywords: surface morphology, Al$_2$O$_3$, microtexture, wettability, hydrophilic, hydrophobic, processing, roughness, mold steel

1. Introduction

Conventionally, the surface finishing of metal molds is always done by hand lapping after processing and/or electrical discharge machining in order to attain small surface roughness without microcracks. However, in this process, operator shortcomings cause these manual processing methods to have a number of limitations. Meanwhile, consistency and repeatability are also required. Consequently, the process is extremely time consuming, which leads to high cost [1].

While automated processes suitable for the finishing of closed dies, they are limited in their application. For example, precision machining using a single point diamond tool is slow, requires conditions not readily available in an industrial environment, and is limited to flat surfaces [2–4]. Chemical micromachining and electrochemical micromachining are limited in their application and can be difficult to control [4–9]. The laser has also been widely used as a machine tool to modify the surface of the engineering materials, such as laser surface alloying, laser cladding, surface texturing, laser physical vapor deposition, laser polishing, etc. [2, 10–20].

Ultimately, surface modifications or surface treatments are vitally important for increasing service life of the critical components and devices used for engineering and structural functions. Numerous surface engineering approaches are employed such as thermal, chemical, mechanical, as well as hybrid treatments to improve or vary/change the surface finish.

In this study, the influence of alumina-based surface processing on the micro-texture, morphology, and wetting behavior of mold steel has been investigated. The morphology of initial as well as processed surfaces was investigated as a function of processing time. After being processed, the influence of processing time on the surface morphology of mold steel was studied by 3D profilometer and scanning electron microscope (SEM). The wettability of the processed surface is also investigated.

2. Materials and methods

2.1 Materials

The chemical composition of mold steel tool steel is shown in **Table 1**.

2.2 Methods

The materials were processed into 25 mm × 25 mm × 5 mm slabs and carefully cleaned with acetone and pure ethyl alcohol to remove any contaminants on its surface.

The planetary mono mill "Pulverisette 6" (Made in Germany) was used for surface processing in the stainless steel processing bowl (volume: 500 ml). The process was performed under the vacuum to prevent contaminations for time periods ranging between 15 and 180 min at a processing speed of 250 rpm. All the processed

Element	C	Si	Mn	Cr	W	V	Fe
(wt.%)	0.9	0.3	1.2	0.5	0.5	0.1	Bal.

Table 1.
Chemical composition of mold steel.

Figure 1.
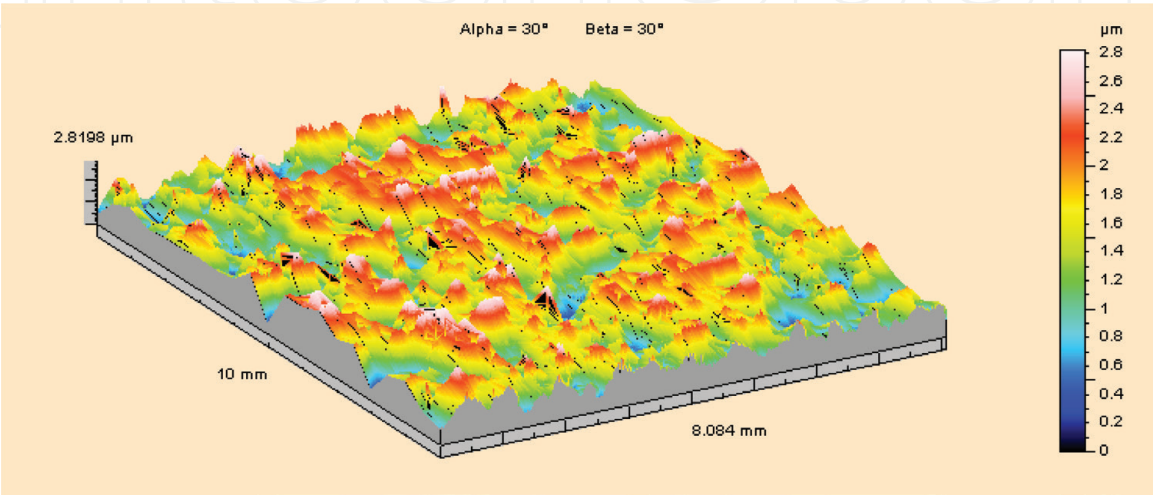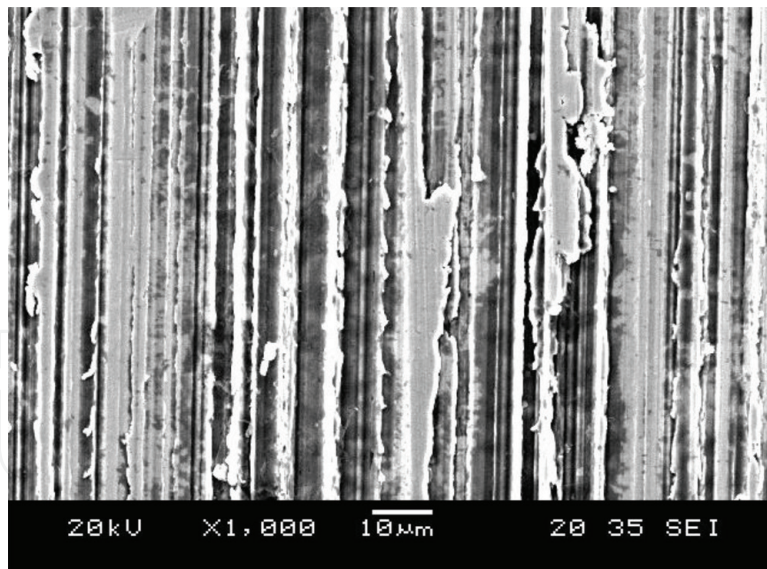*Morphology of the original surface of mold steel.*

Figure 2.
SEM of the initial mold steel surface.

specimens were ultrasonically cleaned in an acetone bath for 10 min with 28–34 Hz frequency and carefully dried. The surface morphology of surfaces was observed by Taylor Hobson profilometer/Talysurf PGI, optical microscope (OM), and scanning electron microscope (SEM) JEOL/JSM-5600. Contact angle (CA) measurement was taken by an advanced contact angle goniometer with DROPimage Advanced (ramé-hart Model 500) attached with a charge-coupled device video camera (with a resolution of 768 × 494 active pixel) and an environmental chamber with temperature control. The volume of the droplet was 10 μL.

Figure 1 shows the Talysurf 3D topography of the original mold steel tool steel specimen, while **Figure 2** shows its corresponding 2D SEM morphology.

3. Results and discussion

3.1 Morphology of the processed surface as a function of processing times

3.1.1 Processing time: 15 min

The morphology of the processed surface after 15 min processing is shown in **Figure 3**, and its related SEM image is expressed in **Figure 4**.

The results indicate that the processed surface is smoother than its initial surface (**Figures 1** and **2**). According to **Figures 3** and **4a**, some small ridges were found distributed on the processed surface. The grooves on the surface had disappeared to a certain extent, together with some smaller island-form ridges (such as labels A and B) due to the shorter processing time. The big ridges cannot be detected and the remained chippings disappear (**Figure 2**), resulted in the smooth processed surface as shown in **Figure 4a**.

Moreover, the magnified parts of **Figure 4a** are shown in **Figure 4b** and **c**, and crack can be found on the processed surface as shown in **Figure 4c** (label C) as a result of the effect of processing balls.

3.1.2 Processing time: 30 min

The morphology of the processed surface after 30 min processing time is shown in **Figure 5**, its corresponding texture is shown in **Figure 6a**, and its magnification
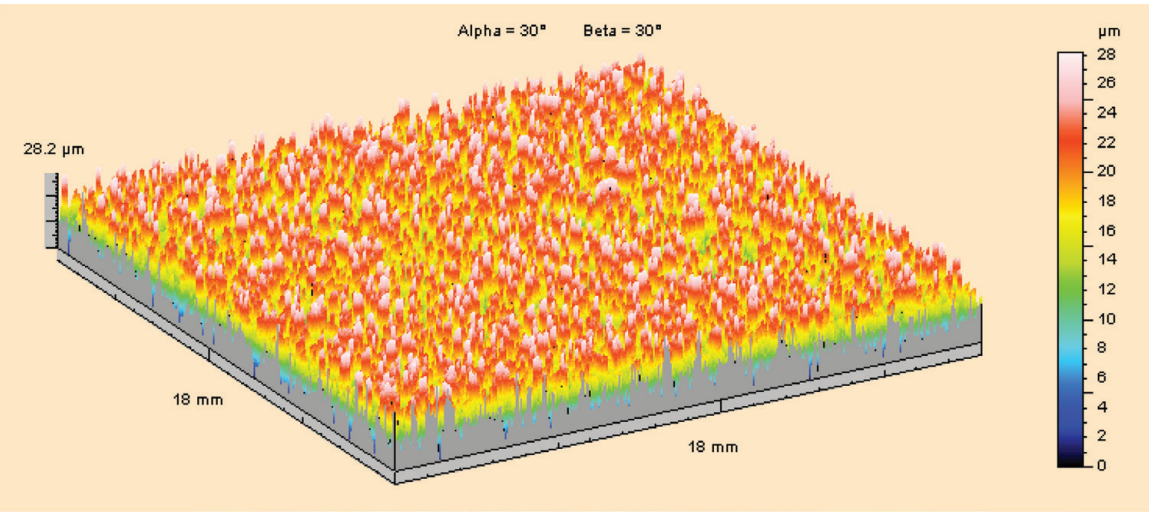
Figure 3.
Morphology of processed surface after 15 min processing time.
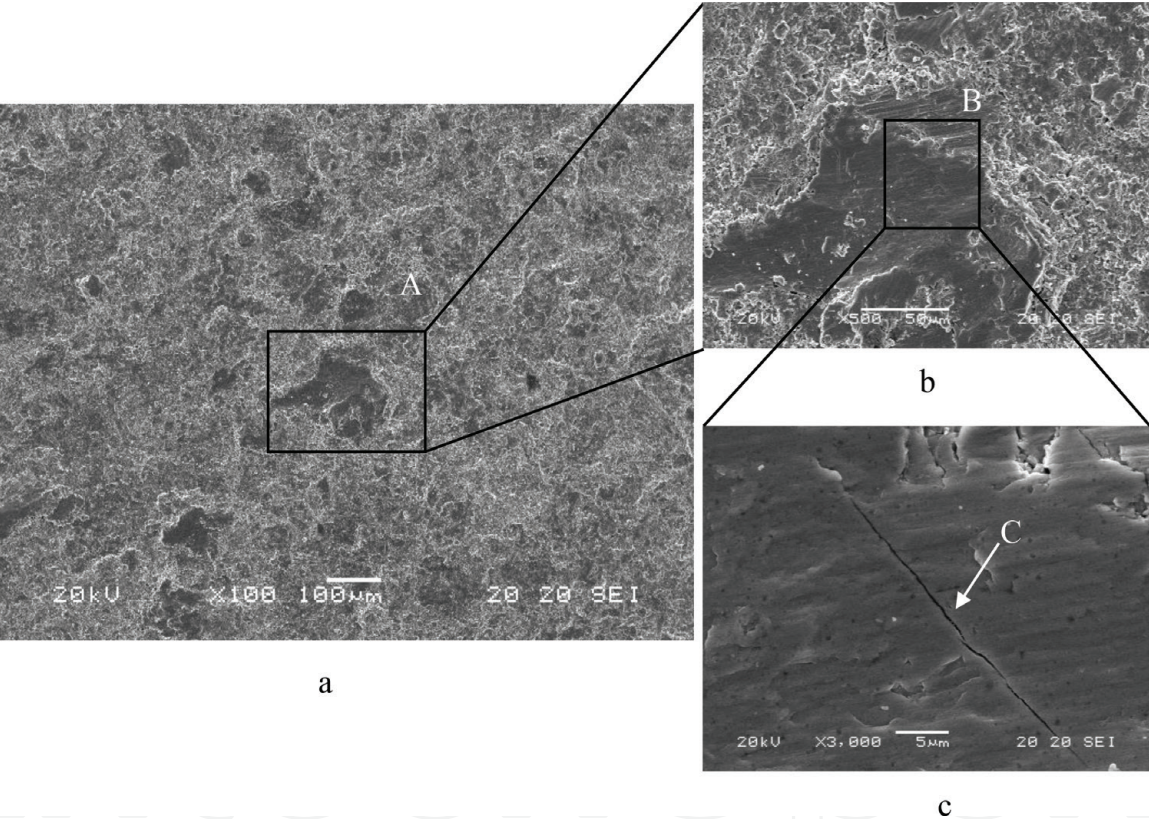

Figure 4.
Processed surface after 15 min processing time.

parts are shown in **Figure 6b** and **c**. Although processing balls remove most high plateaus from the original surface of the specimens (cf. **Figures 2** and **6**), the island-form ridges were found to be still distributed on the processed surface. As expressed in **Figure 6b** and **c**, micropits and cracks can be observed on the surface of the substrate because the balls did not mill sufficiently.

3.1.3 Processing time: 60 min

With the increase of processing time, the processed surface becomes more and more smooth as shown in **Figure 7**, and the formed ridges become smaller and
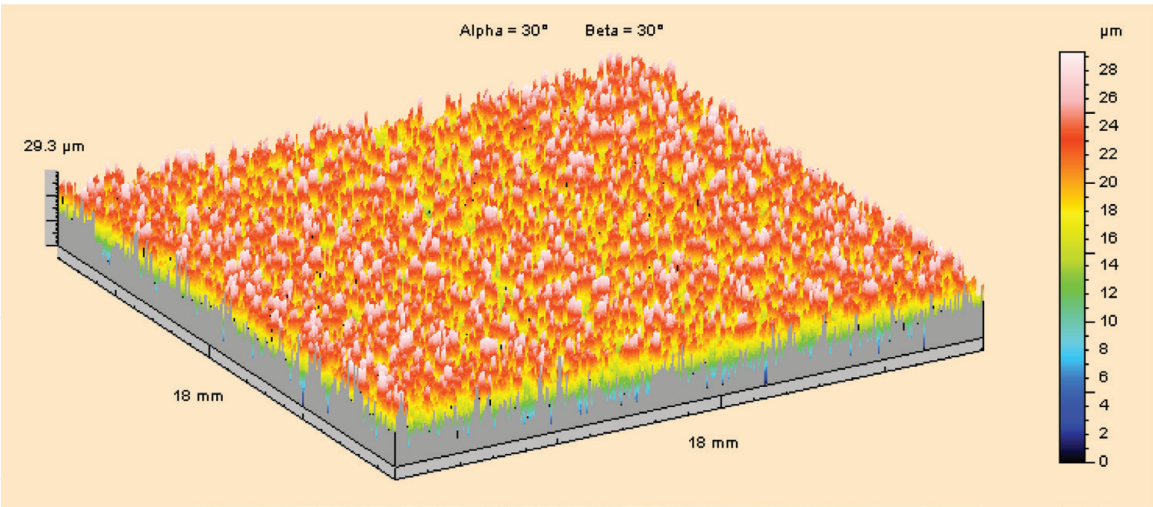
Figure 5.
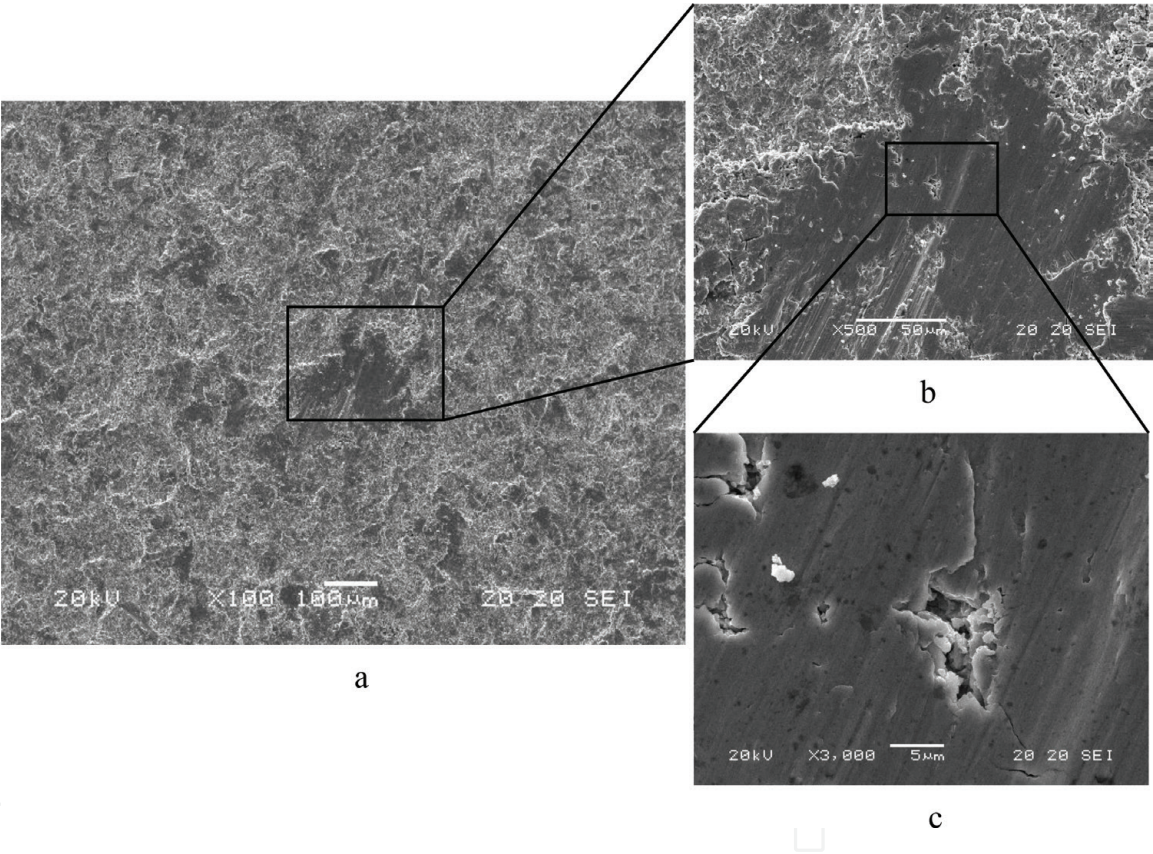*Morphology of processed surface after 30 min processing time.*

Figure 6.
Processed surface after 30 min processing time.

distribute uniformly as shown in **Figure 8** where the magnifications of **Figure 8a** are shown in **Figure 8b** and **c**. It illustrates the uniform changes of the surface topography after 60 min processing time. The variation of the topography of the surface processed at 60 min is distinct. It is observed that the mold steel surface was processed effectively without any defects (cf. **Figures 4, 6**, and **8**).

Generally, increase in processing time simultaneously improves the properties of the surface substrate. However, too longer processing time will be likely to destroy the surface of the substrate which subsequently changes the surface topography and mechanical properties of the steel specimens.
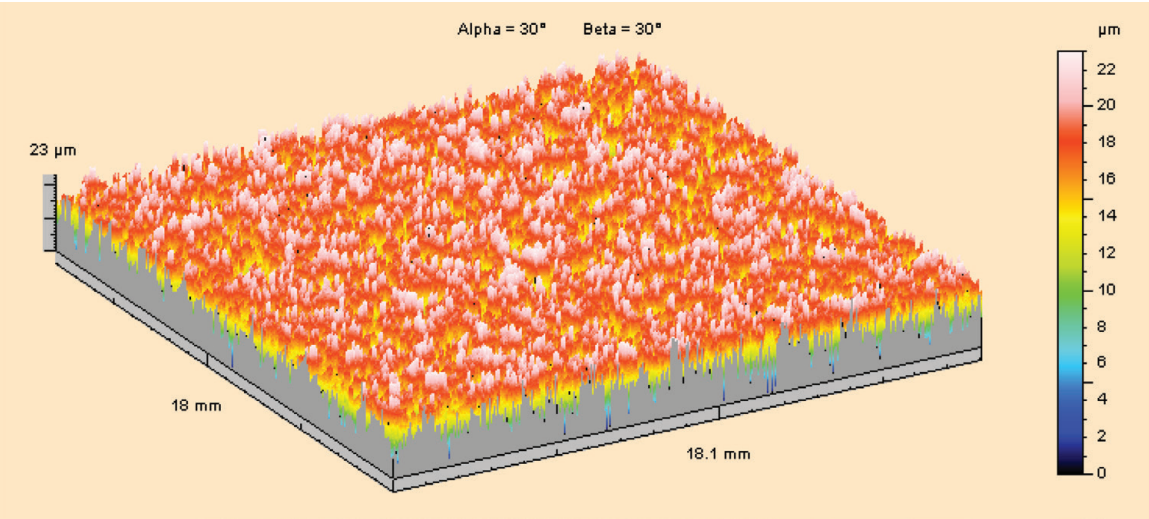
Figure 7.
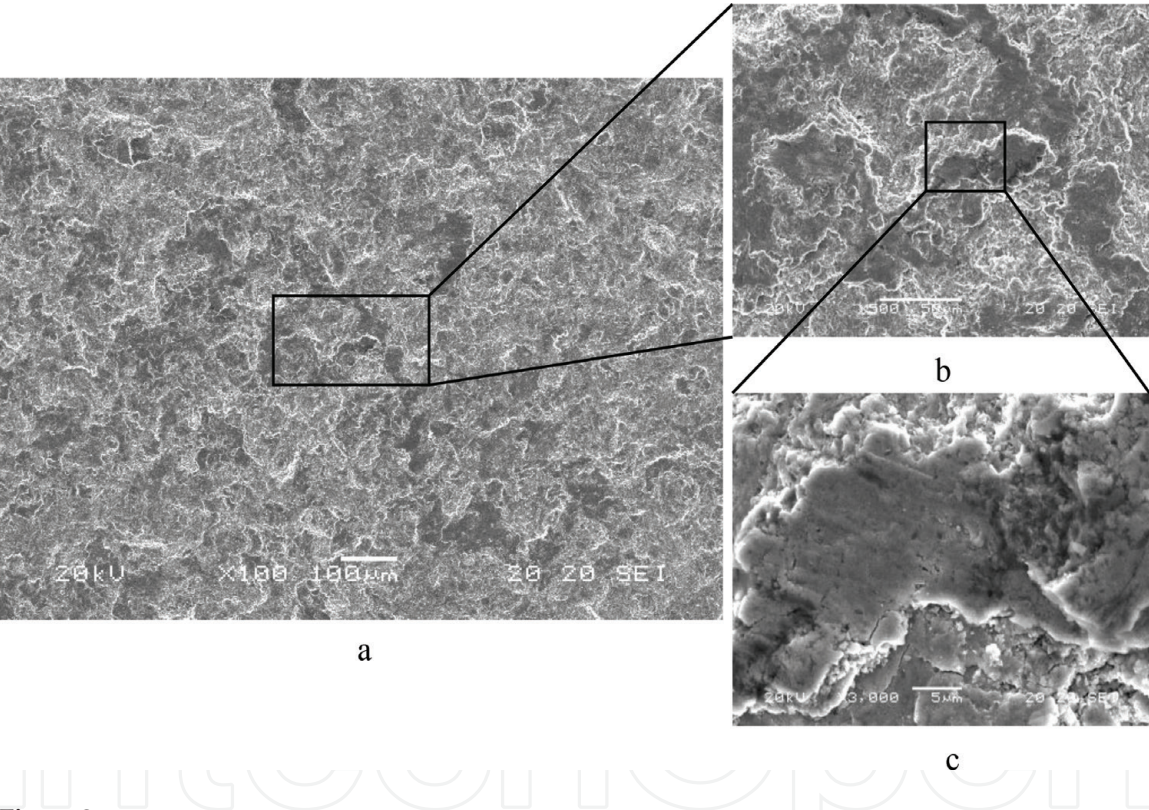*Morphology of processed surface after 60 min processing time.*

Figure 8.
Processed surface after 60 min processing time.

3.1.4 Processing time: 120 min

When compared with the processed surface of 60 min processing time (**Figure 8**), the processed surfaces (**Figures 9** and **11**) of longer processing time give relatively coarser surface. Also, its SEM image (**Figures 10a** and **12a**) and the further magnified counterparts (**Figures 10b, c** and **12b, c**) show the sign of ridges regrowing bigger, some microparticles aggregating loosely, and microcracks scattering on the processed surface. Such surface topography with scattering of microaggregation and micro ball-like amorphous features (**Figure 10c**) implies that there is some level of change of properties of the mold steel surface. This change is not really anticipated since it is initially expected that the properties of the processed surface topography would be the same as its as-received condition or higher than the initial one.
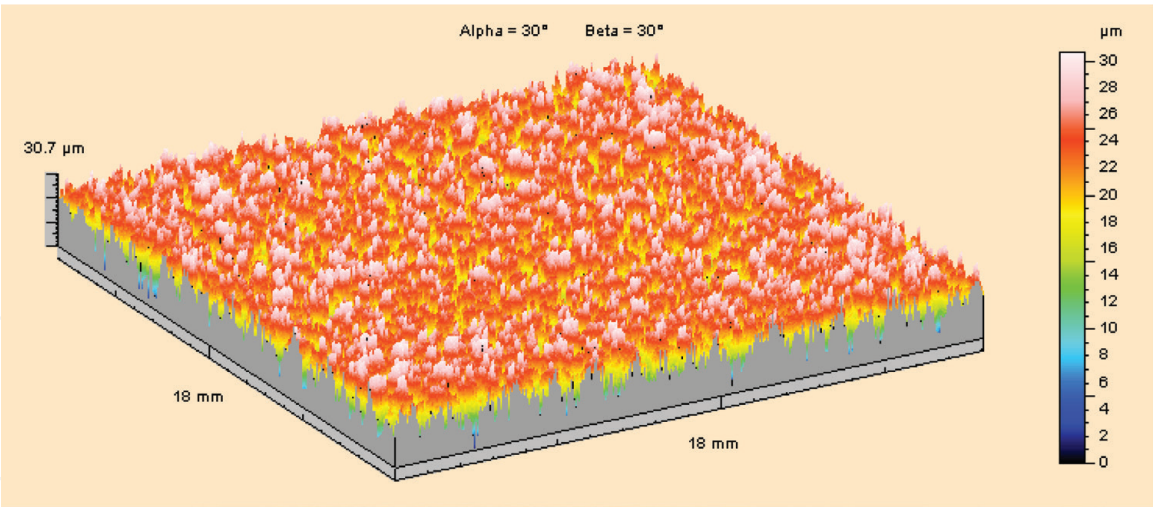
Figure 9.
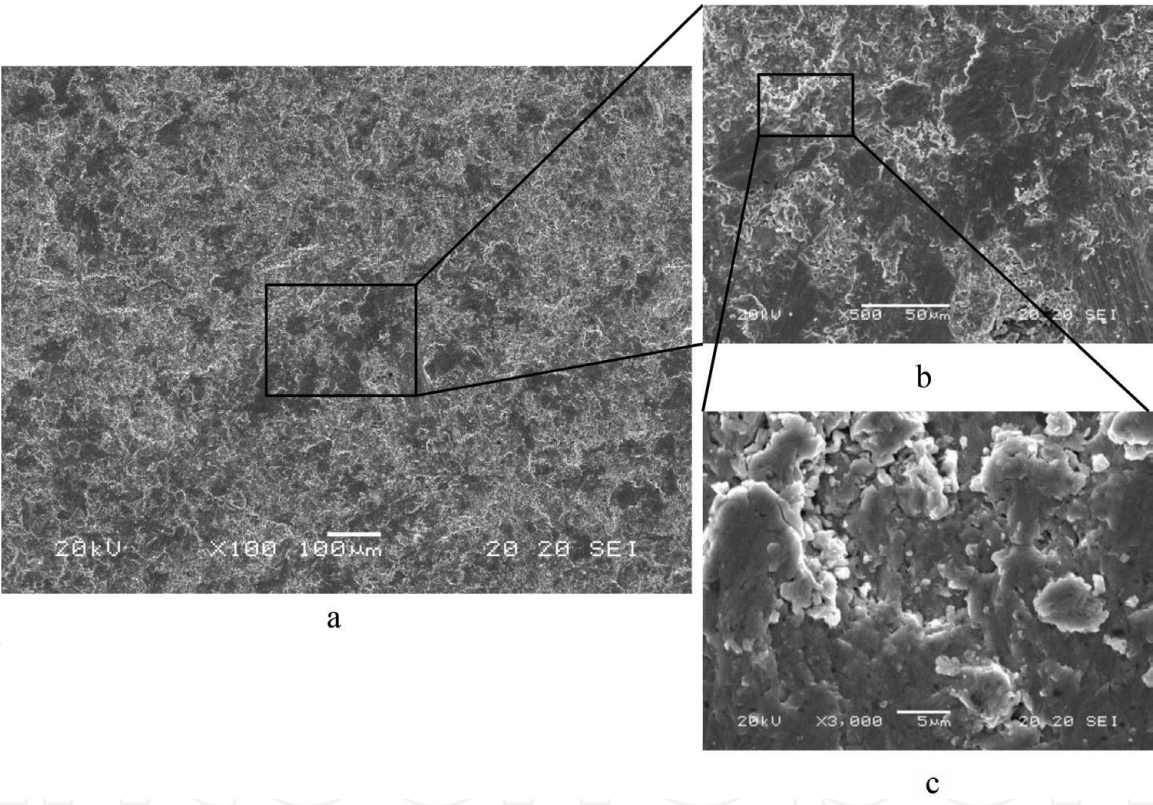*Morphology of processed surface after 120 min processing time.*

Figure 10.
Processed surface after 120 min processing time.

3.1.5 Processing time: 180 min

A longer processing time (i.e., 180 min), besides the morphology of the processed surface changes obviously (**Figure 11**), relatively more severe cracks appear as shown in **Figure 12b** and **c**, which are likely to change the properties of the initial surface drastically.

3.2 Determination of surface roughness

Figure 13 shows the relationship between the arithmetic mean surface roughness *R*a and the processing time. Results indicate that the initial increase in processing
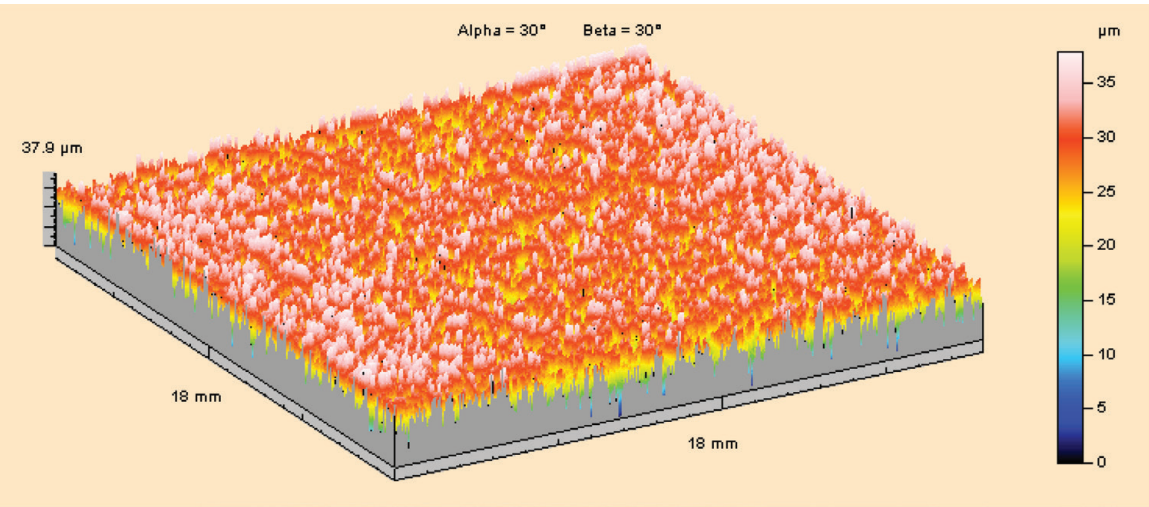
Figure 11.
Morphology of processed surface after 180 min processing time.
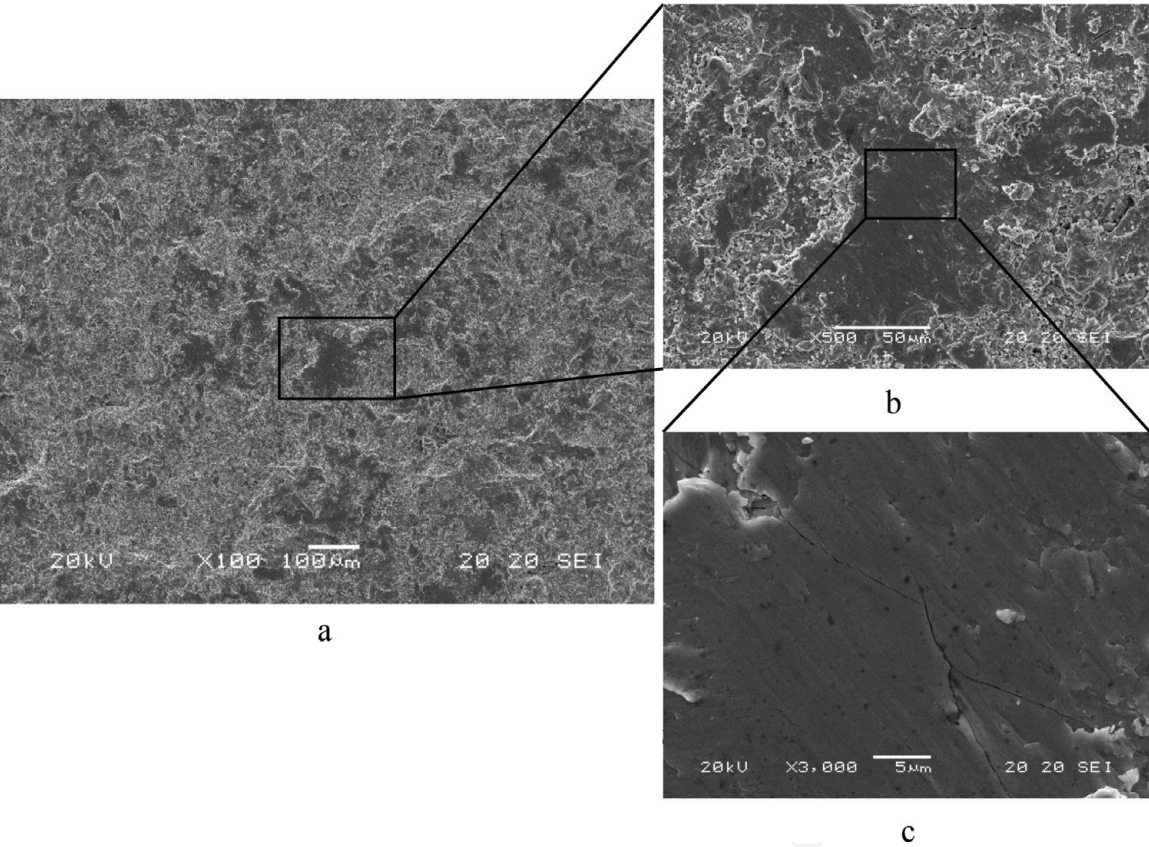

Figure 12.
Processed surface after 180 min processing time.

time accompanies with the increase in surface roughness until the processing time reaches 60 min at which the surface roughness is the minimum. Then, a further increase in the processing time increases the roughness once again which agrees well with morphology as shown in **Figures 3–12**.

3.3 Wettability of milled surface

The variation of CA during the processing process is shown in **Figures 14** and **15**. It is noted that the evolution of CA is related to the processing time. For the initial surface of mold steel, its wettability is hydrophilic. When the processing
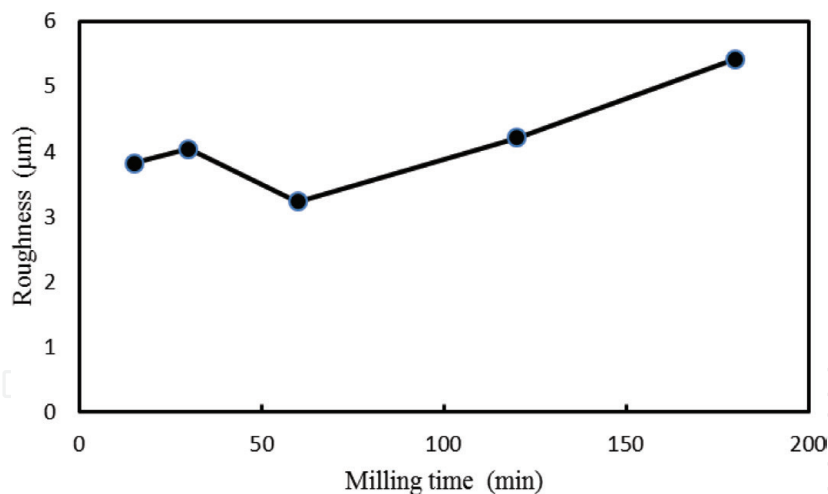
Figure 13.
Correlation between Ra and processing time.

increases, the wettability of the surface varies obviously. The wettability changes from hydrophilic to hydrophobic when the processing time is 60 min, which is an attractive characteristic potential for model release. Moreover, CA increases with the increment of processing time at the early processing period. However, when the surface is processed with longer time, such as 120 and 180 min, the wettability of the surface will be hydrophilic again as shown in **Figure 15**.

It is well known that there is a distinction between the "actual surface" of an interface and the "geometric surface," which is measured in the plane of the interface. At the surface of any real solid, the actual surface will be greater than the geometric surface because of surface roughness. Due to this distinction, the contact angle will be influenced by the roughness. When the surface roughness is considered, the contact angle and droplet profile will change to keep the equilibrium. To evaluate the effect of roughness on surface wettability and calculate the new contact angle of θ' on the rough surface, two different models were proposed by Wenzel and Cassie-Baxter. Both models emphasize on the geometry feature of solid surfaces that acts as a critical factor in determining the wettability.

A system with a droplet placed on a rough solid surface is considered as shown in **Figure 16**, in which the surface texture feature size is much smaller than the droplet, so the influence of liquid weight on an indentation can be neglected when compared to that from surface tension. In traditional theory, whether air can be trapped between liquid and the solid surface is determined by the surface tension of liquid. The liquid intends to exhibit its intrinsic contact angle ($\theta 0$) on the edge of islands. On a hydrophilic substrate ($\theta 0 < 90°$), concave menisci form in the indentations, and the result of liquid surface tension is directed downward and drives the liquid to fill the indentations as much as possible, as shown in **Figure 16a**. On the other hand, for a hydrophobic substrate ($\theta 0 > 90°$), convex menisci form, and the surface tension of liquid is directed upward and pushes the liquid to be suspended on indentations, as shown in **Figure 16b**. Considering of that θ_w is smaller than θ_0 for hydrophilic materials and θ_c is larger than θ_0 for hydrophobic materials, as a result, on an ideal patterned surface, the contact angle would always decrease when $\theta 0 < 90°$ and be increased when $\theta 0 > 90°$. Therefore, one can make the option of the processing time with the ideal surface property according to the practical applications.

3.4 Preliminary computations

During the processing process, the mean value of the magnitude of the critical torque $\tau_{critical}$ can be expressed as:

$$\overline{\tau_{critical}} = \lambda_{\tau} d_t \left[\!\left[F_n + 3 f_{adhesion} \right]\!\right] \qquad (1)$$

where λ_t is a constant in the range $0.5 < \lambda_t < 1$, d_t is the distance parallel to the plane from the center to one of the asperities in contact, $f_{adhesion}$ is an adhesive force at each contact, and F_n is the normal body forces.

$$\overline{\varnothing_{critical}} = \lambda_{\varnothing} \frac{2 \left(\dfrac{3|P + f_{adhesion}|}{4 E^* \sqrt{R^*}} \right)^{\frac{2}{3}}}{3 d_t} \qquad (2)$$
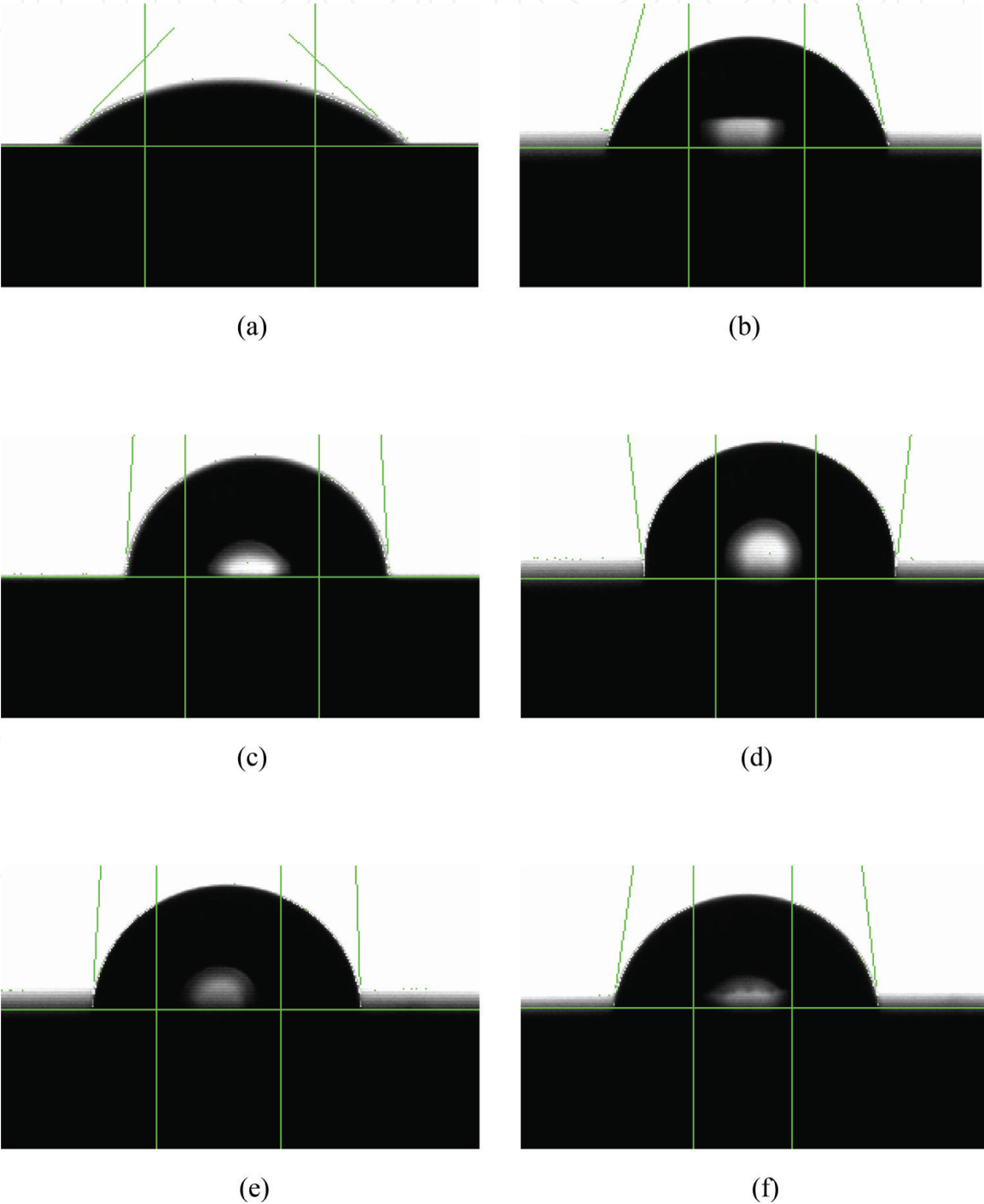
(a)

(b)

(c)

(d)

(e)

(f)

Figure 14.
Variation of contact angle (CA) at different processing times. (a) CA of the initial mold steel surface, (b) CA of the surface at 15 min processing time, (c) CA of the surface at 30 min processing time, (d) CA of the surface at 60 min processing time, (e) CA of the surface at 120 min processing time, and (f) CA of the surface at 180 min processing time.
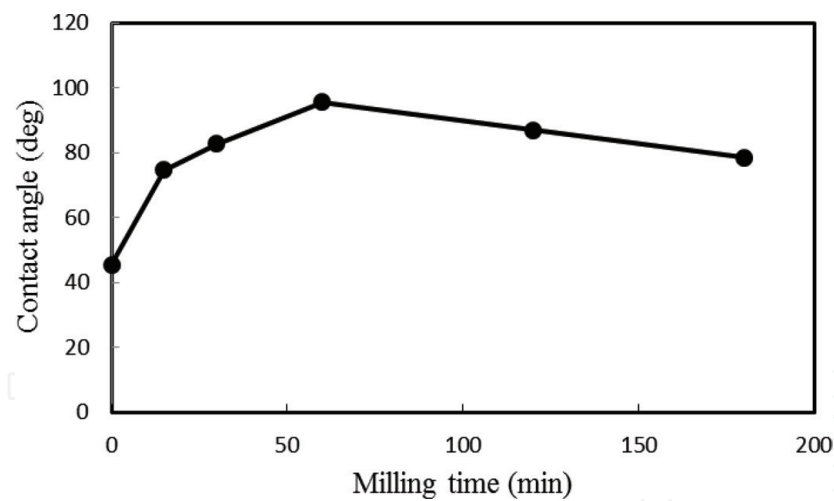
Figure 15.
Correlation between CA and processing time.
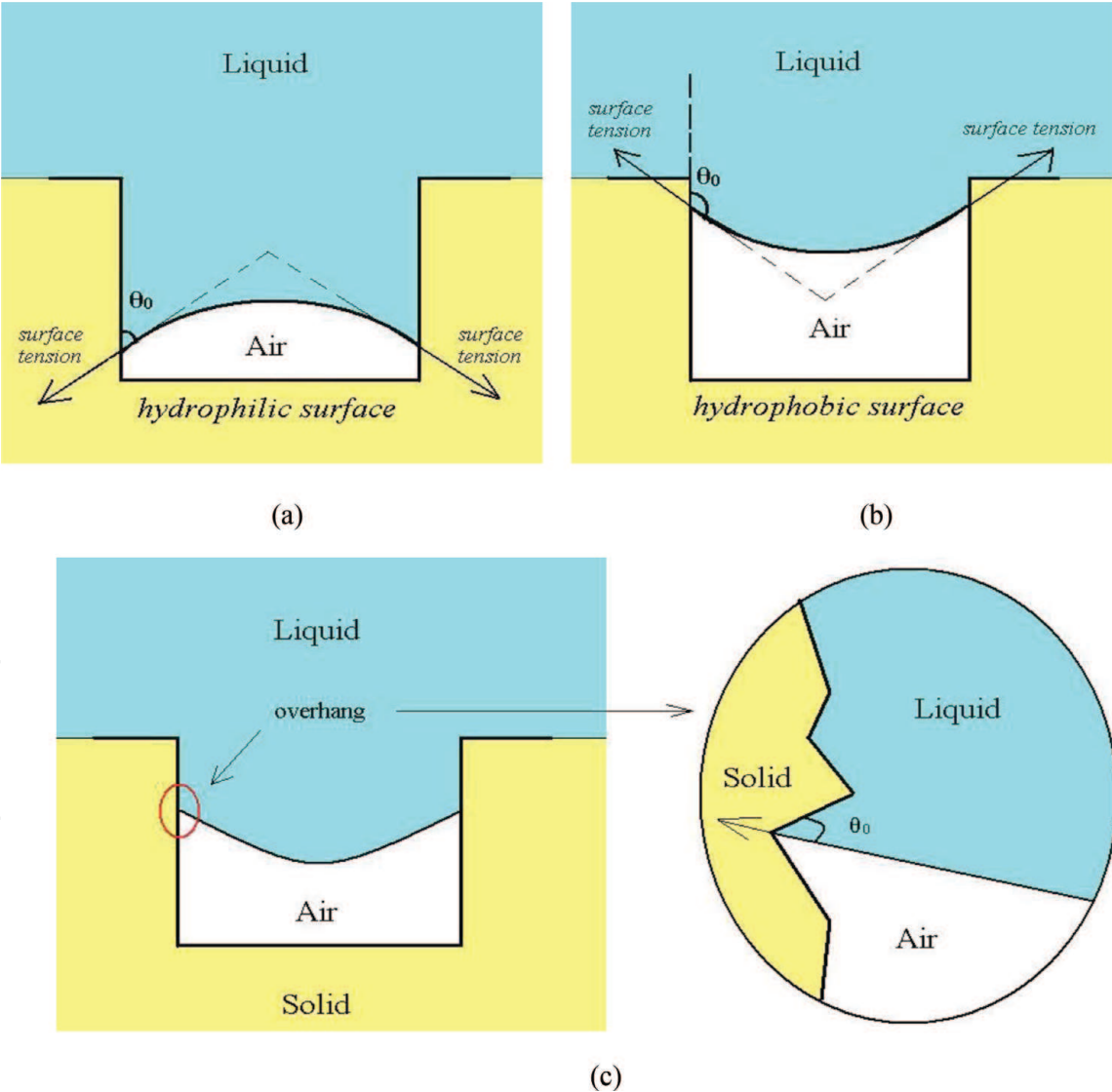

(a)

(b)

(c)

Figure 16.
Schematic representation of the cross section of the droplet-substrate system in indentations. (a) Hydrophilic substrate, (b) hydrophobic substrate, and (c) overhang on a hydrophilic surface with microscopic roughness.

$\overline{\varnothing_{critical}}$ is the critical angle at which critical torque $\overline{\tau_{critical}}$ occurs, $0.63 < \lambda_\varnothing < 1$, P is the total load, $R^* = \dfrac{R_1 R_2}{R_1 + R_2}$ is the reduced radius, and $E^* = \dfrac{E_1 E_2}{E_1(1 - v_2^2) + E_2(1 - v_1^2)}$ is the reduced elastic modulus.

$$\overline{\tau_{decelerating}} = -\gamma\omega \tag{3}$$

where $\gamma = -2\xi\eta_n|d_t|^2 n_{2\pi}$.

$\overline{\tau_{decelerating}}$ is the decelerating torque, ξ is the coefficient ($\xi < 1, or\ \xi \ll 1$), η_n is the damping coefficient, ω is the angular velocity, $n_{2\pi}$ is the number of asperities per revolution, and γ is the adhesive force.

The model consists of expressions for the critical angle and torque at which a ball starts to mill, as well as the rate at which they decelerate. Because of the stochastic nature of surface roughness, it is impossible to accurately reproduce all behavior in a model simple enough to be used in the ball processing phenomena reconstructions. While average processing effect can be accurately replicated, the contact between a real ball and the substrate will not necessarily follow this average due to the details of the geometry. However, in a system of many balls, it is often the case that the average behavior dominates. While variations around the average may have a large effect on the motion of each individual ball, the statistical behavior of a system of many balls will not be significantly changed. The model has been derived for the contact between a ball and a plane. The contact forces in contacts between two balls will be different, and effects such as interactions between asperities make the system far more complex, but the general principle upon which the model is based still applies. The proposed model can provide an adequate approximation of processing effects in the surface processing when torque is dominated by the largest scale of roughness.

4. Conclusions

The morphology of mold steel varies with the different processing times. Increase in processing time simultaneously makes the wettability of processed surface changed from hydrophilic to hydrophobic. Meanwhile, the initial increase in processing time accompanies with the increase in surface roughness until the processing time reaches 60 min at which the surface roughness is the minimum. However, with the increment of processing time, the wettability of the surface will be hydrophilic again. What is more serious is that longer processing time will be likely to destroy the surface of the substrate which subsequently changes the surface morphology and mechanical properties of the steel specimens, which is not really anticipated since it is initially expected that the properties of the processed surface morphology would be the same as its as-received condition or higher than the initial one, especially during the mold releasement.

Author details

Kelvii Wei Guo
Department of Mechanical and Biomedical Engineering, City University of Hong Kong, Kowloon, Hong Kong

*Address all correspondence to: yeelikwok@yahoo.com

IntechOpen

References

[1] Maghsoudi K, Jafari R, Momen G, Farzaneh M. Micro-nanostructured polymer surfaces using injection molding: A review. Materials Today Communications. 2017;**13**:126-143

[2] Roberts AG, Krauss G, Kennedy LR. Tool Steels. 5th ed. Ohio: ASM International, Materials Park; 1998

[3] Dehghan-Manshadi A, Bermingham MJ, Dargusch MS, StJohn DH, Qian M. Metal injection moulding of titanium and titanium alloys: Challenges and recent development. Powder Technology. 2017;**319**:289-301

[4] Ryk G, Kligerman Y, Etson I. Experimental investigation of the laser surface texturing for reciprocating automotive components. Tribology Transactions. 2002;**45**(4):444-449

[5] Assarzadeh S, Ghoreishi M. Prediction of root mean square surface roughness in low discharge energy die-sinking EDM process considering the effects of successive discharges and plasma flushing efficiency. Journal of Manufacturing Processes. 2017;**30**:502-515

[6] Shah Mohammadi M, Ghani M, Komeili M, Crawford B, Milani AS. The effect of manufacturing parameters on the surface roughness of glass fibre reinforced polymer moulds. Composites Part B: Engineering. 2017;**125**:39-48

[7] Wojciechowski S, Maruda RW, Nieslony P, Krolczyk GM. Investigation on the edge forces in ball end milling of inclined surfaces. International Journal of Mechanical Sciences. 2016;**119**:360-369

[8] Vanarase A, Aslam R, Oka S, Muzzio F. Effects of mill design and process parameters in milling dry extrudates. Powder Technology. 2015;**278**:84-93

[9] Brito TG, Paiva AP, Ferreira JR, Gomes JHF, Balestrassi PP. A normal boundary intersection approach to multiresponse robust optimization of the surface roughness in end milling process with combined arrays. Precision Engineering. 2014;**38**(3):628-638

[10] Tangwarodomnukun V. Cavity formation and surface modeling of laser milling process under a thin-flowing water layer. Applied Surface Science. 2016;**386**:51-64

[11] Ahmed Obeidi M, McCarthy E, Brabazon D. Methodology of laser processing for precise control of surface micro-topology. Surface and Coatings Technology. 2016;**307**:702-712

[12] Gisario A, Puopolo M, Venettacci S, Veniali F. Improvement of thermally sprayed WC–Co/NiCr coatings by surface laser processing. International Journal of Refractory Metals and Hard Materials. 2015;**52**:123-130

[13] Vilar R, Sharma SP, Almeida A, Cangueiro LT, Oliveira V. Surface morphology and phase transformations of femtosecond laser-processed sapphire. Applied Surface Science. 2014;**288**:313-323

[14] Yilbas BS, Khaled M, Abu-Dheir N, Aqeeli N, Furquan SZ. Laser texturing of alumina surface for improved hydrophobicity. Applied Surface Science. 2013;**286**:161-170

[15] Guo KW, Tam HY. Study on polishing DF2 (AISI O1) steel by Nd:YAG laser. Journal of Materials Science. 2012, 2012;**1**(1):54-77. DOI: 10.5539/jmsr.v1n1p54

[16] Guo W, Hua M, Tse PW-T, Mok ACK. Process parameters selection for laser polishing DF2 (AISI O1) by Nd:YAG pulsed laser using orthogonal

design. The International Journal of Advanced Manufacturing Technology. 2012;**59**(9-12):1009-1023. DOI: 10.1007/s00170-0113558-1

[17] Kelvii Wei GUO. Effect of polishing parameters on morphology of DF2 (AISI-O1) steel surface polished by Nd:YAG laser. Surface Engineering. 2009;**25**(3):187-195

[18] Wei GUO. Effect of irradiation parameters on morphology of polishing DF2 (AISI-O1) surface by Nd:YAG laser. Advances in Materials Science and Engineering. 2007;**3**:5-9. DOI: 10.1155/2007/51316

[19] Lugomer S. Laser Technology-Laser Driven Processes. Englewood Cliffs, NJ, USA: Prentice Hall Inc; 1990. pp. 419-439

[20] Steen WM. Laser Material Processing. 3rd ed. London: Springer-Verlag; 2003